J Nanopart Res (2019) 21: 176
https://doi.org/10.1007/s11051-019-4619-x

RESEARCH PAPER

A wide solar spectrum light harvesting Ag_2Se quantum dot-sensitized porous TiO_2 nanofibers as photoanode for high-performance QDSC

Nisha Singh · Vignesh Murugadoss · Jeniffa Rajavedhanayagam · Subramania Angaiah

Received: 8 March 2019 / Accepted: 24 July 2019 / Published online: 10 August 2019

Abstract A wide spectrum of light harvesting silver selenide (Ag_2Se) quantum dots (QDs) with an average size of ~ 5 nm has been synthesized by a low-temperature one-pot hot injection method. To finely control the size of Ag_2Se QDs, oleylamine was used as the solvent, and dodecanethiol was used as the capping agent as well as a stabilizer. The prepared Ag_2Se QDs were ex situ sensitized on the porous TiO_2 nanofiber (NF) substrate via a direct adsorption method to use as efficient photoanode for quantum dot-sensitized solar cell (QDSC). The UV-Vis-NIR absorption and photoluminescence studies revealed that Ag_2Se QD-sensitized porous TiO_2 NF photoanode (Ag_2Se/P-TiO_2) exhibited near-infrared (NIR) absorption and fast electron kinetics. Further, the QDSC fabricated using Ag_2Se/P-TiO_2 NFs as the photoanode, Cu_2S as the counter electrode, and liquid polysulfide (S^{2-}/S_x^{2-} redox couple) as the electrolyte exhibited a photoconversion efficiency of 2.50% with an improved photocurrent density of 11.12 mA/cm^2.

Keywords Electrospinning · Ag_2Se quantum dots · TiO_2 nanofibers · Quantum dot-sensitized solar cell

N. Singh · V. Murugadoss · J. Rajavedhanayagam · S. Angaiah (✉)
Electro-Materials Research Laboratory, Centre for Nanoscience and Technology, Pondicherry University, Puducherry 605014, India
e-mail: a.subramania@gmail.com

Introduction

Quantum dot-sensitized solar cells (QDSCs) have garnered immense interest on account of the ability of quantum dots that elicited a theoretical efficiency up to ~ 44%. This higher efficiency (more than the Shockley-Queisser limit (~ 31%)) is attributed to the unique optical properties of QDs such as bandgap tuning by size control, large dipole interaction, resistivity to photobleaching, high extinction coefficient, and multiple exciton generations by means of impact ionization (Kamat 2013; Kouhnavard et al. 2014). The steady progress in the class of QDs has mainly focused on binary QDs to explore as sensitizers in QDSCs. Cd- and Pb-based QDs such as CdSe (Gao et al. 2009), CdS (Lai et al. 2014), and PbSe (Benehkohal et al. 2012) have been studied extensively as sensitizers; however, its practical applicability inflicts the resolution of a green and clean world. Hence, replacement with environment benign QDs has to turn into the trend in QDSCs. In addition to toxicity issue, the broad light absorbing range, high CB edge position than semiconductor metal oxide, and adsorption of maximum QDs over the photoanode substrate are the relevant factors need to focus on. In this aspect, a low toxic Ag_2Se QDs came into attention due to its narrow bandgap (~ 0.15 eV) which could capable to absorb more solar flux from the visible to the near-infrared region (Sahu et al. 2012; Langevin et al. 2013). The small size of Ag_2Se QDs would also help to tune the conduction band edge and cause fast electron transfer to the CB of semiconductor oxide film substrate (Kamat 2008). Suitability of

Ag_2Se QDs as the sensitizer has been studied by Tubtimtae et al., where Ag_2Se QDs is found to achieve low efficiency of 1.57%. This low performance of Ag_2Se QD-based QDSC might have contributed to in situ sensitization of QDs over the TiO_2 NP film and electron hopping while carrying to the external circuit of the device. The slow electron transport, electron-hole recombination, and poor coverage of QDs on the photoanode can be overcome by employing Ag_2Se QDs over the porous TiO_2 NFs for proper adsorption of Ag_2Se QDs on the surface of the photoanode substrate.

The in situ sensitization such as chemical bath deposition (CBD) and successive ionic layer adsorption and reaction (SILAR) for QDs adsorption has found the cause for lower photoconversion efficiency in the QDSCs due to the wide range of size distribution and disparity in desire morphology, whereas an ex situ sensitization method encourages the formation of small-sized QDs and tuning of bandgap as well (Lai et al. 2014). Most of the ex situ adsorption are done by using a bilinker agent like 3-mercaptopropionic acid (MPA), while few preferred to anchor via direct adsorption method, where direct adsorption has the advantage of maximum adsorption on the surface of photoanode and fast electron transport kinetics in comparison with the assistance by bilinker agent (Pernik et al. 2011).

In order to increase the photocurrent density of QDSCs, the maximum uptake of QDs over the photoanode substrate have been made to prevent the electron-hole recombination. The porous TiO_2 NF-based photoanode has offered a better way to improve the power conversion efficiency of QDSC; this would accommodate the high quantity of QDs over the surface by providing high surface area and proper contact between the counter electrode and electrolyte. Electrospun TiO_2 NFs have the higher surface area for superior adsorption of QDs and faster semidirected electron transport and lesser transit time to the FTO plate in addition to internal light scattering, and the highly fibrous structure which facilitates higher electrolyte uptake than the conventional nanoparticle morphology.

In the present investigation, we prepared Ag_2Se QDs by a simple hot injection method at a low temperature using 1-DDT as a capping agent. Later, these QDs are directly adsorbed on the porous TiO_2 NFs in a solvent medium. Finally, the optical and photovoltaic performances of Ag_2Se QD-sensitized porous TiO_2 NF-based photoanode for QDSC are studied in detail.

Experimental

Materials

Titanium IV isopropoxide (TiP, 99%), polyvinyl pyrrolidone (PVP, $M_w = 1{,}300{,}000$), silver chloride (AgCl, 99.9%), selenium powder (99.9%), oleylamine (technical grade, 70%), and 1-dodecanethiol (> 98%) were procured from Sigma-Aldrich. Methanol (> 99.5%), ethanol (> 99%), hexane (> 95%), acetic acid glacial (99–100%), and glycerol (GR 87%) were purchased from Merck India Ltd. and used without further purification.

Synthesis of Ag_2Se QDs

Ag_2Se QDs were prepared by a simple hot injection method using oleylamine as the solvent and dodecanethiol as the effective capping agent as well as a stabilizer for the reaction to control the particle size. The synthesis was carried out in two steps. First, selenium precursor solution was prepared in which 2 mM of Se powder in 10 mL of oleylamine was taken in a two-neck round-bottom flask and then refluxed at 150 °C for 1 h to form Se-OAm complex. Second, 0.4 mM of silver precursor, 5 mL of OAm (solvent), and 1 mL of 1-DDT (capping agent) were taken in a 50-mL round-bottom flask and heated initially up to 130 °C under N_2 gas atmosphere. At this temperature, the preprepared OAm-Se complex solution was injected into the flask under continuous stirring for 15 min. In this condition, it starts the process of nucleation and growth which led to the formation of quantum dots that was evident by the change in color from yellow to the dark gray. Later, the reaction was stopped, and then, the solution was left for cooling followed by precipitation by adding 10 mL of cold methanol. The pure QDs were obtained after centrifugation using by ethanol and methanol as the solvent, and then they were dispersed in a nonpolar solvent (hexane).

Preparation of Ag_2Se-sensitized porous TiO_2 NFs

The highly porous TiO_2 NFs were prepared by the solvosonication process by dispersing conventional TiO_2 NFs in glycerol as a pore-forming solvent. The ultrasonication (Leela Sonic, 50 W and 30 kHz) was done for 90 min. Then, the TiO_2 NFs are removed from glycerol and calcined at 300 °C for 10 min in a muffle

furnace to get highly porous TiO_2 NFs. This porous TiO_2 NF has interconnected porous structure with higher porosity and surface area than the conventional TiO_2 NFs (Nisha Singh et al. 2018).

The porous TiO_2 NF paste was then prepared by mixing 30 wt% of porous TiO_2 NFs with terpineol (50 wt%), dibutyl phthalate (5 wt%), and ethyl cellulose (15 wt%) in ethanol. The FTO glass substrates (12 Ω sq^{-1}) were thoroughly rinsed with deionized water, acetone, and ethanol in an ultrasonic bath for 5 min and dried in a hot air oven. The prepared porous TiO_2 NF paste was coated on pretreated FTO substrates by a doctor blade technique using adhesive scotch tape so that the thickness was maintained at 11–12 μm and then the coatings were sintered at 450 °C for 30 min and cooled to 80 °C. The coated substrate was then dipped in Ag_2Se QDs colloidal solution (prepared from 5 mg QDs dispersed in 5 mL of hexane) for 24 h to complete the adsorption of Ag_2Se QDs onto the porous TiO_2 NF-based photoanode. The resultant photoanode was finally rinsed with hexane and then dried.

Physical characterization

The phase purity and crystal structure of prepared Ag_2Se QDs and Ag_2Se QD-sensitized porous TiO_2 NFs were confirmed by X-ray diffraction analysis (Rigaku, Ultima IV) using Cu-Kα source over the scan range of 20–80° with an increment of 0.02°. The particle size of Ag_2Se QDs was confirmed by the dynamic light scattering (DLS) technique (Malvern Panalytical), and the attachment of Ag_2Se QDs on the porous TiO_2 NFs was confirmed by transmission electron microscope (JEOL, FEG-TEM, JSM-7600F) with selected area electron diffraction (SAED) pattern. The morphological analysis with the elemental composition of Ag_2Se QDs and Ag_2Se QD-sensitized porous TiO_2 NFs was determined by using scanning electron microscopy (Hitachi, model: S-4200) coupled with energy-dispersive X-ray spectrometer (EDX).

The absorbance spectra were recorded at 300–1200 nm using UV-Vis-NIR spectrophotometer (PerkinElmer, model: L-650) for Ag_2Se QDs and Ag_2Se QD-sensitized porous TiO_2 NFs. Photoluminescence studies were performed using a luminescence spectrometer (NanoLog, HORIBA Jobin Yvon) with xenon lamp as the source of excitation for Ag_2Se QDs and Ag_2Se QD-sensitized porous TiO_2 NFs.

The performance of fabricated Ag_2Se QD-sensitized porous TiO_2 NF-based QDSCs was determined by a calibrated AM 1.5 solar illumination (Newport, Oriel Instruments, USA; 150 W, model: 67005) with a light intensity of 100 $mWcm^{-2}$ calibrated using standard silicon solar cell (Newport, Oriel Instruments, model: 91150 V) and a computer-controlled digital source meter (Keithley, model: 2420). Electrochemical AC impedance measurements (Biologic VSP, France) were carried out under AM 1.5 sun illumination at room temperature in the frequency range of 1 mHz to 100 kHz with an AC amplitude of 10 mV (Subramania et al. 2015)

Fabrication of QDSC devices

The photoanode was prepared as in the "Preparation of Ag_2Se-sensitized porous TiO_2 NFs" section, and the counter electrode was prepared by mixing 95 wt% of Cu_2S nanoparticles with 5 wt% N-methyl-2-pyrrolidone (binder) and coated on pretreated FTO glass plates by the doctor blade technique and then dried at 80 °C for overnight in a vacuum oven to remove excess solvents. The prepared photoanode and the counter electrode were sealed using 60-μm surlyn hot melt spacer, and the space of cell was filled with polysulfide redox electrolyte containing 2 M Na_2S, 2 M S, and 0.2 M KCl in 3:7 (v/v) mixture of methanol and deionized water through the predrilled holes in the counter electrode. Later, the holes were closed by using a surlyn strip and left as such for few hours so that complete diffusion of the electrolyte into both electrodes takes place. The active area of the cell was 0.30 cm^2.

Results and discussion

Characterization of Ag_2Se QDs

The X-ray diffraction (XRD) pattern of prepared Ag_2Se QDs is shown in Fig. 1. Its characteristic peaks resemble the orthorhombic low-temperature β-phase of Ag_2Se (Hu et al. 2000) This is well matched with the JCPDS Card No. 024-1041. No significant peaks corresponding to the organic ligands are observed. The peak at $\theta = 29.9°$ (represented by *) does not match with any silver selenide pattern (Panneerselvam et al. 2009). The broadening of XRD peaks is attributed to the smaller size of Ag_2Se QDs. It has been reported that organic ligands play a significant role in the stability of the quantum dots

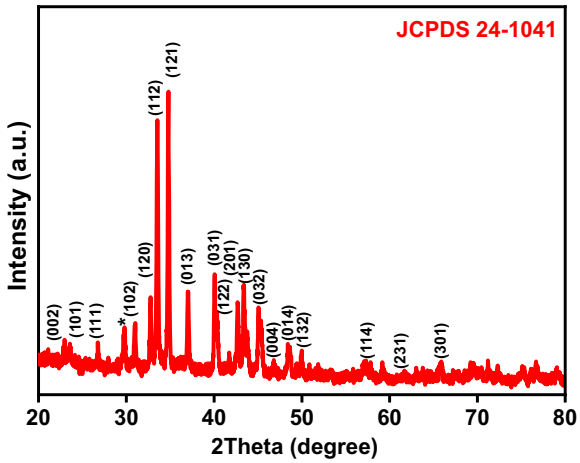

Fig. 1 XRD pattern of Ag_2Se QDs

(Chen et al. 1997; Wickham et al. 2000). On nucleation of Ag_2Se QDs, the organic ligands bound on its surface and the smaller Ag_2Se QDs would be formed with the broadened XRD peaks (Xing et al. 2008). The transmission electron microscopy (TEM) image (Fig. 2a) confirms that the Ag_2Se quantum dots have an average size of ~5 nm. Figure 2 b shows the lattice fringe that represents the (004) plane corresponding to 0.195 nm lattice spacing. These results confirm the formation of Ag_2Se QDs.

The Ag_2Se QDs size was further confirmed from DLS analysis, and its histogram is shown in Fig. 2c. The average size of Ag_2Se QDs is 5 nm. The EDX spectrum of Ag_2Se is shown in Fig. 2d. It gives information on the elemental composition of Ag_2Se QDs, and the stoichiometric ratio of silver/selenide is found to be 1.98 which is close to the standard 2:1 ratio of Ag_2Se.

The optical absorption spectrum recorded for Ag_2Se QDs dispersed in hexane is shown in Fig. 3a, and its Tauc plot is calculated to determine the bandgap of obtained absorbance from 400 to 1100 nm. The absorption spectrum exhibits the characteristic excitonic peak at 826 nm which is a low-energy peak of Ag_2Se QDs and attributes blue shift from the bulk Ag_2Se. The excitonic peak shows the existence of fewer surface defects which is prerequisite criteria of an efficient sensitizer for QDSC (Jara et al. 2014). The resolved feature of blue shifting towards lower wavelength represents the quantum confinement effect of Ag_2Se QDs. From the Tauc plot, the optical bandgap of 1.15 eV is calculated by using the energy relation of $(\alpha h\nu)^2$ vs $h\nu$, where α is the absorption coefficient and $h\nu$ is photon energy. This extended absorption to NIR region will help to amplify in harvesting more photons from the solar spectrum and generate more electron-hole pairs upon illumination, and hence, such QDs own wide solar absorption capability and can be used as an efficient sensitizer for QDSC.

Photoluminescence study is carried out for Ag_2Se QDs as shown in Fig. 3b. It shows a discernible

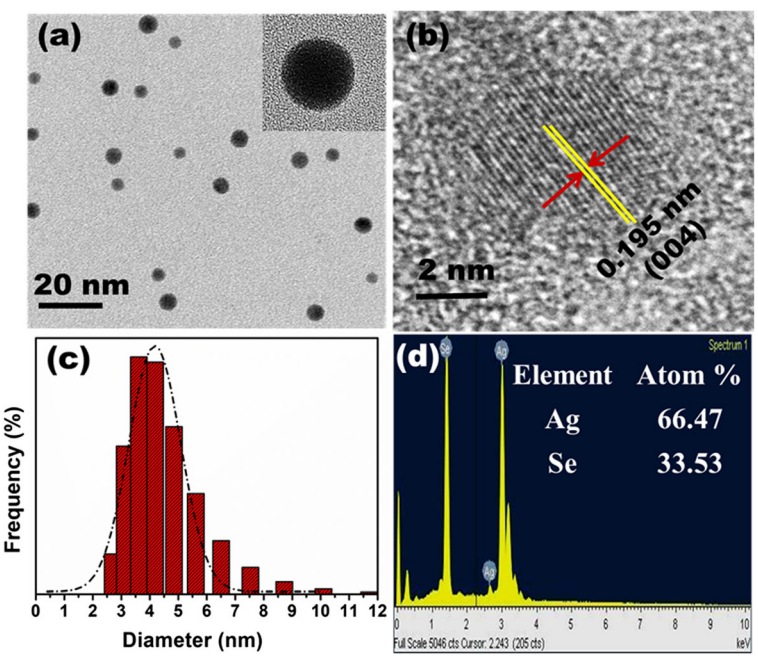

Fig.2 **a**, **b** TEM images of Ag_2Se QDs. **c** Histogram of Ag_2Se QDs from DLS analysis. **d** EDX spectrum of Ag_2Se QDs

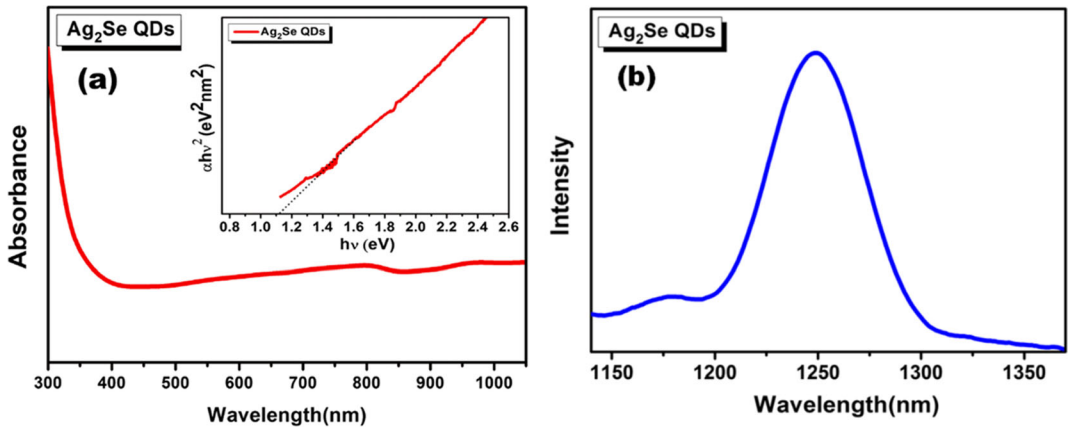

Fig.3 **a** UV-Vis-NIR absorption spectrum with inset Tauc plot of Ag_2Se QDs. **b** Photoluminescence spectrum of Ag_2Se QDs

emission peak at 1249 nm in the narrow range from 1200 to 1300 nm. The calculated FWHM for the emission peak was found to be 52 nm. This clearly shows the narrow size distribution of Ag_2Se QDs. In addition, sharp emission intensity attributes to the less density of defect sites (Cao and Che 2014), thereby Ag_2Se QDs can be proved efficient in improving photovoltaic performance as QDs inbuilt with the low defect and high PL emission quality. The appearance of small shoulder peak along with the main emission line may be due to the transition from a selenium vacancy that acts as a donor for Ag_2Se. (U. N. Roy et al. 2005)

Characterization of Ag_2Se QD-sensitized porous TiO_2 NFs

The XRD pattern of Ag_2Se QD-sensitized porous TiO_2 NFs is studied to investigate the presence of ex situ adsorbed Ag_2Se QDs onto the porous TiO_2 NFs, and it is previously sensitized using the direct ex situ direct adsorption method (Pernik et al. 2011). Figure 4 shows the XRD patterns of porous TiO_2 NFs and Ag_2Se QD-sensitized porous TiO_2 NFs, where diffraction peaks of porous TiO_2 NFs clearly indexed to the anatase phase structure. The TiO_2 NFs being porous in nature have shown the enhanced adsorption of Ag_2Se QDs on TiO_2 photoanode that can be seen from the XRD pattern. Along with the peaks of TiO_2 NFs, there are eight major peaks of Ag_2Se QDs such as (102), (120), (112), (121), (013), (031), (113), and (032) that were observed which justify the adsorption of Ag_2Se QDs over the TiO_2 NF-based photoanode. Moreover, broadening in the XRD peaks is due to the existence of small sizes of TiO_2 nanoparticles composed of TiO_2 NFs and QDs as well (Wei et al. 2015).

Figure 5 a illustrates the UV-Vis-NIR absorbance spectra of porous TiO_2 NFs with and without sensitized Ag_2Se QDs. The plain porous TiO_2 NFs show the absorbance onset > 400 nm due to possible better light harvesting as a consequence of porous nature of TiO_2 NFs which tend to increase light scattering effect inside the TiO_2 NFs (Bijarbooneh et al. 2013). On the other side, the enhancement in the absorption covers a wide range from 400 to 1100 nm compared with porous TiO_2 NFs confirm the complete adsorption of Ag_2Se QDs on TiO_2 NF-based photoanode. The corresponding optical bandgap was calculated by Tauc plot as shown in Fig. 5b and found the decreased bandgap

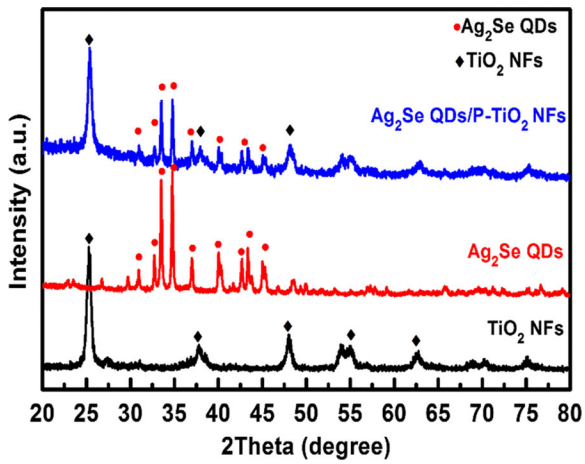

Fig. 4 XRD pattern of Ag_2Se QD-sensitized porous TiO_2 NF-based photoanode

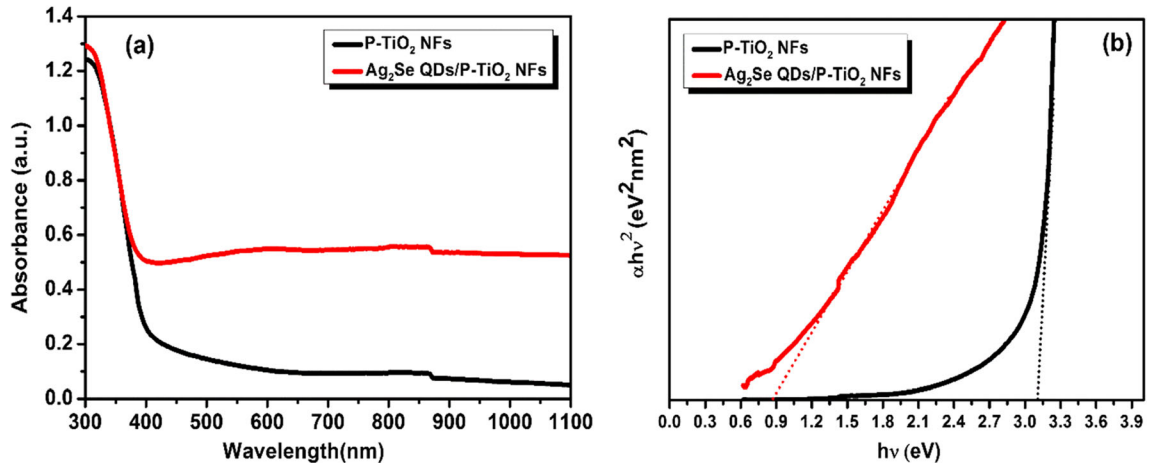

Fig. 5 **a** UV-Vis-NIR absorption spectra and **b** Tauc plots of porous TiO_2 NFs and Ag_2Se QD-sensitized porous TiO_2 NF-based photoanodes

of 0.91 eV for Ag_2Se QD-sensitized porous TiO_2 NF-based photoanode. Therefore, it remarkably improved absorption suggesting Ag_2Se QDs as a promising sensitizer for QDSC.

It can be seen from Fig. 6 that the separation of photogenerated electron holes and their kinetics was investigated by photoluminescence (PL) studies. The photoluminescence emission peak occurs at 392 nm for porous TiO_2 NFs when excited by 325-nm wavelength attributes the indirect band-to-band transition of the TiO_2 (Abazovic et al. 2006). Ag_2Se QD-sensitized porous TiO_2 NF photoanode shows emission at the same wavelength as that of TiO_2 NFs but with the significant quenching in the intensity of the emission peak. The quenching of the intensity indicates the reduced electron-hole recombination and efficient electron transfer from the CB of Ag_2Se QDs to the CB of TiO_2 NFs which forms a hybrid nanostructure.

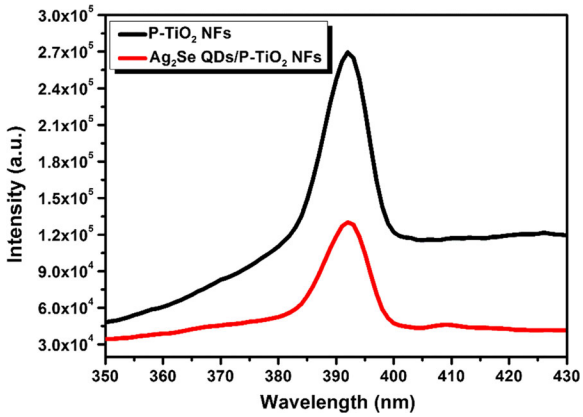

Fig. 6 Emission spectra of porous TiO_2 NFs and Ag_2Se QD-sensitized porous TiO_2 NFs

Thus, the PL spectra proved the charge separation by increasing the driving force of extracted electrons, and it suggests the higher conduction band of Ag_2Se QDs due to quantum confinement effect (Gao et al. 2009; Cao et al. 2015). Therefore, these extracted electrons would improve the photocurrent efficiency of the QDSC.

Figure 7a and b show the HR-TEM image of Ag_2Se QD-sensitized porous TiO_2 NFs in which porous TiO_2 NFs can be seen with the diameter ~ 95 nm composed of a network of TiO_2 nanoparticle size of < 10 nm. Here, it is clear that Ag_2Se QDs (about ~ 5 nm) are tethered over the porous TiO_2 NFs. The observed lattice spacings of 0.323 nm and 0.210 nm of Ag_2Se QDs that correspond to the planes (112) and (204), respectively, confirm the adsorption of Ag_2Se QDs over the TiO_2 NFs. The diffraction rings in the selected electron diffraction are shown in Fig. 7c, and they match well with (211) and (101) planes of TiO_2 and (004) and (020) planes of Ag_2Se QDs, respectively. The compositional EDX analysis was carried out on Ag_2Se QD-sensitized TiO_2 NF-based photoanode which is shown in Fig. 7d. It suggests that the Ag_2Se QDs is composed of Ag and Se elements and is homogeneously distributed on the TiO_2 substrate.

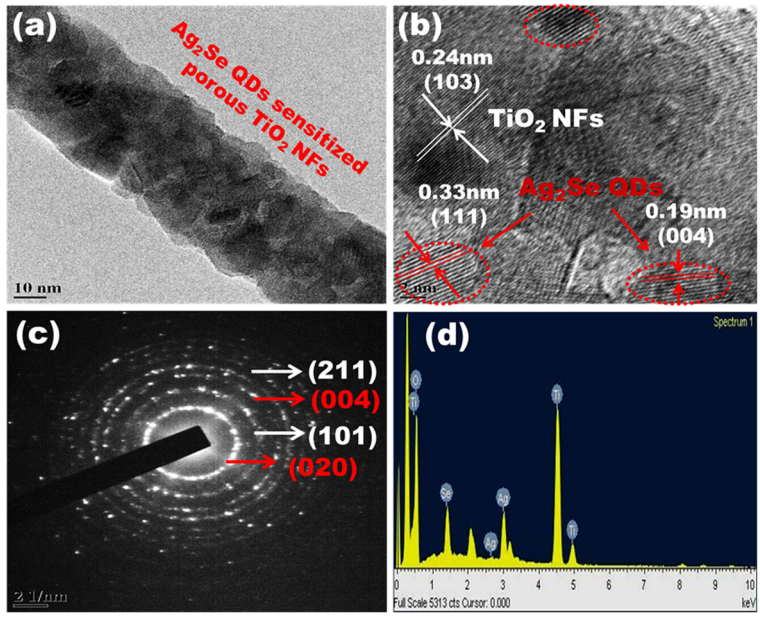

Fig.7 **a**, **b** HR-TEM images of Ag_2Se QD-sensitized porous TiO_2 NFs. **c** SAED pattern. **d** EDX spectrum of Ag_2Se QD-sensitized porous TiO_2 NFs

Photovoltaic performance of QDSC

The photovoltaic performance of fabricated QDSC is evaluated from the photocurrent-voltage (J-V) characteristic measurements which is shown in Fig. 8. Its average photovoltaic parameters from the three tested parallel fabricated QDSCs are given in Table 1. It can be seen from the table that the photovoltaic performance of Ag_2Se QD-sensitized porous TiO_2 NF-based QDSC is increased to 2.50% from 1.79% of conventional TiO_2 NF-based QDSC. This enhancement in the performance is a consequent result of a wide solar absorption from visible to near-infrared region by Ag_2Se QDs that are loaded over the porous TiO_2 NFs. The substantial improvement in the J_{sc} (11.12 mA cm^{-2}) is due to the absorption of narrow size of Ag_2Se QDs that could easily penetrate the porous TiO_2 photoanode and lead to more photogenerated electrons which increase the electron injection to the TiO_2 NFs. It can also be seen that V_{oc} and FF of Ag_2Se QDs sensitized porous TiO_2 NFs photoanode-based QDSC got improvement than that of the conventional TiO_2 photoanode-based QDSC. This is due to the large quantity of Ag_2Se QDs loaded on the porous TiO_2 NFs that helps to elevate the Fermi level of Ag_2Se QDs towards more negative than the TiO_2 NFs. The porous network of TiO_2 NFs offer proper interaction with the polysulfide electrolyte to penetrate inside the TiO_2 NFs. The counter electrode, Cu_2S, is necessary to reduce the oxidized Ag_2Se QDs and prevent the recombination of electrons. Thus, the power conversion efficiency of QDSC obtained using Ag_2Se

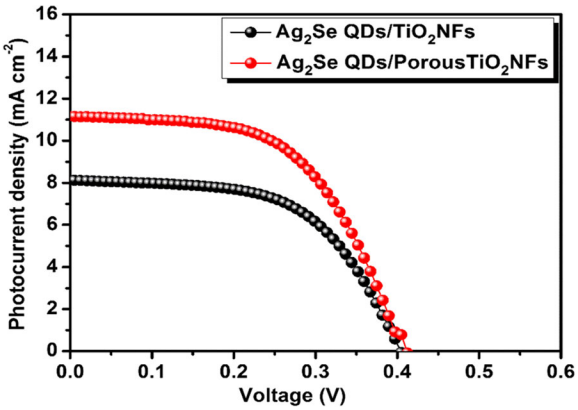

Fig. 8 J-V characteristic curves of Ag_2Se QD-sensitized conventional TiO_2 NFs and porous TiO_2 NF-based QDSCs

Table 1 Photovoltaic parameters of fabricated QDSCs based on Ag_2Se QDs/TiO_2 NFs and Ag_2Se QDs/P-TiO_2 NFs as photoanodes

QDSCs	J_{sc} (mA cm^{-2})	V_{oc} (V)	FF	η%
Ag_2Se QDs/TiO_2 NFs	8.10	0.402	0.552	1.79
Ag_2Se QDs/P-TiO_2 NFs	11.12	0.410	0.550	2.50

Table 2 Comparison of photovoltaic performance of QDSC based on prepared Ag_2Se/TiO_2 with reported Ag_2S/TiO_2-based QDSC

QDSCs	J_{sc} (mA cm^{-2})	V_{oc} (V)	FF	η%	Ref.
Ag_2S QDs/TiO_2 NRs	4.25	0.29	0.330	0.41	(Li et al. 2014)
Ag_2S QDs/TiO_2 NRs	2.30	0.248	0.350	0.78	(Pawar et al. 2017)
Ag_2S QDs/TiO_2 NPs	1.43	0.520	0.470	0.35	(Badawi et al. 2018)
Ag_2Se QDs/P-TiO_2 NFs	11.12	0.410	0.550	2.50	This work

QD-sensitized porous TiO_2 NFs as the photoanode has significant improvement than that obtained using the conventional TiO_2 NFs and the other reported Ag_2S/TiO_2-based QDSCs (Table 2).

Electrochemical AC impedance studies of QDSC

To further understand the electron transport dynamics and charge recombination inside the fabricated QDSC, the impedance measurements were carried out and obtained fitted parameters which are given in Table 3. Figure 9 shows the Nyquist plots obtained for Ag_2Se-sensitized conventional TiO_2 NFs and porous TiO_2 NF-based QDSCs. These plots illustrate the recombination mechanism occurred between Cu_2S/polysulfide electrolyte (R_1) and TiO_2 NFs/Ag_2Se QDs/polysulfide electrolyte (R_2) interfaces in QDSCs. In accordance with the fitted parameters values, the R_2 interface resistance of 147.56 Ω has to exhibit the potential of Ag_2Se QDs in reducing the electron back recombination with the redox couple of electrolyte as Ag_2Se QDs adsorbed sufficiently on the TiO_2 NFs that have reduced grain boundaries for the fast electron transfer without interruption. The resistance at R_2 interface was found to be reduced for Ag_2Se QD-sensitized porous TiO_2 NF-based QDSC that is also in agreement with the improved V_{oc} of 0.410 V in photovoltaic performance. The R_1 (1.18 Ω) of Ag_2Se QD-sensitized porous TiO_2 NF-based QDSC is comparatively less resistance than that of conventional TiO_2 NF-based QDSC. This is due to the porous nature of TiO_2 NFs that provide sufficient surface area to make good contact of polysulfide electrolyte into the TiO_2 NFs to speed up the redox process (Chen et al. 2013).

Table 3 Simulated electrochemical impedance parameters of QDSCs based on Ag_2Se QDs/TiO_2 NFs and Ag_2Se QDs/P-TiO_2 NFs as photoanodes

QDSCs	R_s (Ω)	R_1 (Ω)	R_2 (Ω)
Ag_2Se QDs/TiO_2 NFs	12.37	1.37	182.3
Ag_2Se QDs/P-TiO_2 NFs	11.62	1.18	147.56

Conclusion

In summary, Ag_2Se QDs were successfully synthesized by a one-pot hot injection method with an average size of ~ 5 nm. The prepared Ag_2Se QDs were sensitized on the porous TiO_2 NFs by a direct ex situ method. The optical studies have shown the beneficial scope of Ag_2Se/P-TiO_2 to use as photoanode material for QDSC. This is due to the high surface area of porous TiO_2 NFs and the maximum loading of Ag_2Se QDs. The obtained power conversion efficiency of 2.50% for QDSC fabricated with Ag_2Se QD-sensitized porous TiO_2 NFs brings out that the porous nature of TiO_2 NFs and Ag_2Se QDs is the cause to improve the photocurrent density of QDSC. The combination of a wide solar spectrum light harvester, Ag_2Se QDs as the sensitizer with porous TiO_2 NFs as the photoanode, would open more opportunities in QDSC research.

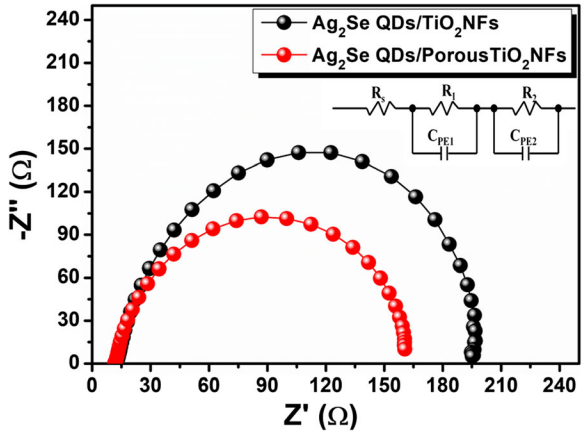

Fig. 9 Nyquist plots of Ag_2Se QD-sensitized conventional TiO_2 NFs and porous TiO_2 NF-based QDSCs

Funding information The authors gratefully acknowledge the CSIR, New Delhi, for providing the financial support (No. 01/2810/14/EMR-II dated 24-11-2014) and the CIF Pondicherry University for providing the instrumentation facilities. One of the authors, Ms. Nisha Singh, sincerely thanks the UGC, New Delhi, for providing Research Fellowship under the RGNF scheme.

Compliance with ethical standards

Conflict of interest The authors declare that they have no conflicts of interest.

References

Abazovic ND, Comor MI, Dramicanin MD, Jovanovic DJ, Ahrenkiel SP, JMN (2006) Photoluminescence of anatase and rutile TiO_2 particles. J Phys Chem B 110:25366–25370. https://doi.org/10.1021/jp064454f

Badawi A, Mostafa NY, Al-hosiny NM et al (2018) The photovoltaic performance of Ag_2S quantum dots-sensitized solar cells using plasmonic Au nanoparticles/TiO_2 working electrodes. Mod Phys Lett B 1850172:1–17. https://doi.org/10.1142/S0217984918501725

Benehkohal NP, Boix PP, Chavhan S, Demopoulos GP (2012) Colloidal PbS and PbSeS quantum dot sensitized solar cells prepared by electrophoretic deposition. J Phys Chem C 116:16391–16397

Bijarbooneh FH, Zhao Y, Sun Z, Heo YU, Malgras V, Kim JH, Dou SX (2013) Structurally stabilized mesoporous TiO_2 nanofibres for efficient dye-sensitized solar cells. APL Mater 1:32106–32107

Cao Q, Che R (2014) Synthesis of near-infrared fluorescent, elongated ring-like Ag_2Se colloidal nanoassemblies. RSC Adv 4:16641. https://doi.org/10.1039/c4ra00613e

Cao Q, Cheng Y-F, Bi H, Zhao X, Yuan K, Liu Q, Li Q, Wang M, Che R (2015) Crystal defect-mediated band-gap engineering: a new strategy for tuning the optical properties of Ag_2Se quantum dots toward enhanced hydrogen evolution performance. J Mater Chem A 3:20051–20055. https://doi.org/10.1039/C5TA04978D

Chen C-C, Herhold AB, Johnson CS, Alivisatos AP (1997) Size dependence of structural metastability in semiconductor nanocrystals. Science (80) 276:398 LP-401. https://doi.org/10.1126/science.276.5311.398

Chen H, Zhang T, Fan J et al (2013) Electrospun hierarchical TiO_2 nanorods with high porosity for efficient dye-sensitized solar cells. ACS Appl Mater Interfaces 5:9205–9211

Gao X, Li H, Sun W et al (2009) CdTe quantum dots-sensitized TiO_2 nanotube array photoelectrodes. J Phys Chem C 113:7531–7535. https://doi.org/10.1021/jp810727n

Hu J, Deng B, Lu Q et al (2000) Hydrothermal growth of b -Ag_2Se tubular crystals. Chem Commun 8:715–716. https://doi.org/10.1039/a909785f

Jara DH, Yoon SJ, Stamplecoskie KG, Kamat PV (2014) Size-dependent photovoltaic performance of $CuInS_2$ quantum dot-sensitized solar cells. Chem Mater 26:7221–7228. https://doi.org/10.1021/cm5040886

Kamat PV (2008) Quantum dot solar cells. Semiconductor nanocrystals as light harvesters. J Phys Chem C 112:18737–18753

Kamat PV (2013) Quantum dot solar cells. The next big thing in photovoltaics. J Phys Chem Lett 4:908–918

Kouhnavard M, Ikeda S, Ludin NA, Ahmad Khairudin NB, Ghaffari BV, Mat-Teridi MA, Ibrahim MA, Sepeai S, Sopian K (2014) A review of semiconductor materials as sensitizers for quantum dot-sensitized solar cells. Renew Sust Energ Rev 37:397–407. https://doi.org/10.1016/j.rser.2014.05.023

Lai L-H, Protesescu L, Kovalenko MV, Loi MA (2014) Sensitized solar cells with colloidal PbS-CdS core-shell quantum dots. Phys Chem Chem Phys 16:736–742. https://doi.org/10.1039/c3cp54145b

Langevin M, Lachance-quirion D, Ritcey AM (2013) Size-dependent extinction coefficients and transition energies of near-infrared β-Ag_2Se colloidal quantum dots. J Phys Chem C 117:5424–5428

Li W, Yang J, Liu M, Luo Y, Xiao Y, Fu L, Wu S (2014) Electrochemical atomic layer deposition of Ag_2S quantum dots sensitized TiO_2 nanorods array photoanodes and Cu_2S counter electrode for solar cells. J Electrochem Soc 161:510–514. https://doi.org/10.1149/2.0501410jes

Panneerselvam A, Nguyen CQ, Malik MA, O'Brien P, Raftery J (2009) The CVD of silver selenide films from dichalcogenophosphinato and imidodichalcogenodiphosphinatosilver (I) single-source precursors. J Mater Chem 19:419–427. https://doi.org/10.1039/b812074a

Pawar SA, Patil DS, Hyeok J et al (2017) Quantum dot sensitized solar cell based on TiO2/CdS/Ag_2S heterostructure. Opt Mater (Amst) 66:644–650. https://doi.org/10.1016/j.optmat.2017.03.011

Pernik DR, Tvrdy K, Radich JG, Kamat PV (2011) Tracking the adsorption and electron injection rates of CdSe quantum dots on TiO_2: linked versus direct attachment. J Phys Chem C 115:13511–13519. https://doi.org/10.1021/jp203055d

Roy UN, Cui Y, Miles R, Burger A, Goldstein JT, Bell ZW (2005) Micro-Raman and photoluminescence spectroscopies of horizontal Bridgman-grown $AgGaSe_2$. J Appl Phys 98:1–5. https://doi.org/10.1063/1.2127128

Sahu A, Khare A, Deng DD, Norris DJ (2012) Quantum confinement in silver selenide semiconductor nanocrystals. Chem Commun 48:5458. https://doi.org/10.1039/c2cc30539a

Singh N, Zaahir S, Subasri A, Sivasankar N, Subramania A (2018) Development of porous TiO_2 nanofibers by solvosonication process for high performance quantum dot sensitized solar cell. Sol Energy Mater Sol Cells 179:417–426. https://doi.org/10.1016/j.solmat.2018.01.042

Subramania A, Vijayakumar E, Pratheep P, Sivasankar N, Karthick SN (2015) Influence of PVP template on the formation of porous TiO_2 nanofibers by electrospinning technique for dye-sensitized solar cell. Appl Phys A Mater Sci Process 120:1211–1218. https://doi.org/10.1007/s00339-015-9306-x

Wei L, Li F, Hu S, Li H, Chi B, Pu J, Jian L (2015) CdS quantum dot-sensitized vertical TiO_2 nanorod arrays by a simple linker-assisted SILAR method. J Am Ceram Soc 98:3173–3178. https://doi.org/10.1111/jace.13726

Wickham JN, Herhold AB, Alivisatos AP (2000) Shape change as an indicator of mechanism in the high-pressure structural transformations of CdSe nanocrystals. Phys Rev Lett 84: 923–926

Xing B, Li W, Dou H et al (2008) Systematic study of the properties of CdSe quantum dots synthesized in paraffin liquid with potential application in multiplexed bioassays. JPhysChemC 112:14318–14323